Insights into the mode of inhibition of human mitochondrial monoamine oxidase B from high-resolution crystal structures

Claudia Binda*, Min Li†, Frantisek Hubálek†, Nadia Restelli*, Dale E. Edmondson†‡, and Andrea Mattevi*‡

*Department of Genetics and Microbiology, University of Pavia, 27100 Pavia, Italy; and †Departments of Biochemistry and Chemistry, Emory University, Atlanta, GA 30322

Communicated by Judith P. Klinman, University of California, Berkeley, CA, June 23, 2003 (received for review April 11, 2003)

Monoamine oxidase B (MAO-B) is an outer mitochondrial membrane-bound enzyme that catalyzes the oxidative deamination of arylalkylamine neurotransmitters and has been a target for a number of clinically used drug inhibitors. The 1.7-Å structure of the reversible isatin–MAO-B complex has been determined; it forms a basis for the interpretation of the enzyme's structure when bound to either reversible or irreversible inhibitors. 1,4-Diphenyl-2-butene is found to be a reversible MAO-B inhibitor, which occupies both the entrance and substrate cavity space in the enzyme. Comparison of these two structures identifies Ile-199 as a ''gate'' between the two cavities. Rotation of the side chain allows for either separation or fusion of the two cavities. Inhibition of the enzyme with *N*-(2-aminoethyl)-*p*-chlorobenzamide results in the formation of a covalent N(5) flavin adduct with the phenyl ring of the inhibitor occupying a position in the catalytic site overlapping that of isatin. Inhibition of MAO-B with the clinically used *trans*-2-phenylcyclopropylamine results in the formation of a covalent C(4a) flavin adduct with an opened cyclopropyl ring and the phenyl ring in a parallel orientation to the flavin. The peptide bond between the flavin-substituted Cys-397 and Tyr-398 is in a *cis* conformation, which allows the proper orientation of the phenolic ring of Tyr-398 in the active site. The flavin ring exists in a twisted nonplanar conformation, which is observed in the oxidized form as well as in both the N(5) and the C(4a) adducts. An immobile water molecule is H-bonded to Lys-296 and to the N(5) of the flavin as observed in other flavin-dependent amine oxidases. The active site cavities are highly apolar; however, hydrophilic areas exist near the flavin and direct the amine moiety of the substrate for binding and catalysis. Small conformational changes are observed on comparison of the different inhibitor–enzyme complexes. Future MAO-B drug design will need to consider ''induced fit'' contributions as an element in ligand–enzyme interactions.

The structure and function of monoamine oxidases A and B (MAO-A and -B) have been of interest to a wide variety of scientific disciplines because of the role of these enzymes in the oxidation of arylalkylamine neurotransmitters such as dopamine and serotonin. The proposed role of MAO-B in age-dependent neurodegenerative diseases has resulted in a renewed interest in this enzyme as a target for the development of neuroprotective agents. MAO-B inhibitors are used clinically and others are in development. MAO-A and -B have been extensively investigated and serve as the prototype for the flavin-dependent amine oxidases.

The recent description of the 3.0-Å structure of human recombinant MAO-B in its pargyline-inhibited form by our laboratories (1) revealed a two-domain architecture of the molecule and its mode of binding to the mitochondrial outer membrane through a C-terminal hydrophobic α-helix. These studies show the substrate negotiates a protein loop in its entry into the active site of the enzyme, which involves traversing an ''entrance cavity'' before entering the ''substrate cavity'' (Fig. 1).

We report here the structures of MAO-B in complex with several reversible and irreversible inhibitors (Fig. 2) to elucidate their respective binding modes as well as to provide insights into the mode of inhibition. Higher (1.7 Å) resolution data were obtained that provide additional structural details on the active site relevant to drug design and to the detailed catalytic mechanism.

The structure of MAO-B in complex with isatin was determined because this compound is found at higher levels in patients with neuropathological conditions and has been shown to be a competitive MAO-B inhibitor with a K_i of 3 μM (2). In the course of these studies, we have uncovered a competitive MAO-B inhibitor ($K_i = 35$ μM) that is identified as 1,4-diphenyl-2-butene, a contaminant of polystyrene products (3).

The structure of MAO-B after inhibition with *N*-(2-aminoethyl)-*p*-chlorobenzamide (also known as Ro 16-6491) was elucidated. This compound belongs to a class of highly specific MAO-B inhibitors, which includes lazabemide. A previous study (4) suggested this inhibitor binds to a site on the enzyme other than the flavin moiety. Tranylcypromine (*trans*-2-phenylcyclopropylamine) has been known for >40 years as a MAO inhibitor and used clinically as an antidepressant. As with the lazabemide class of inhibitors, tranylcypromine has been thought to exert its inhibitory action as a mechanism-based inhibitor by covalent binding of the MAO-B-catalyzed reaction product to an amino acid side chain (5, 6). The structural data presented in this study show that, in contrast to previous conclusions, tranylcypromine and *N*-(2-aminoethyl)-*p*-chlorobenzamide inhibit MAO-B by covalent binding to the flavin ring, however, at differing sites on the isoalloxazine ring.

Materials and Methods

Expression, purification, absorption spectral studies, and catalytic assays of recombinant human liver MAO-B were performed as described (7). All chemicals used in this study were obtained from commercial sources.

Orthorhombic MAO-B crystals were grown by the sitting-drop vapor diffusion method at 4°C (1) using polystyrene microbridges obtained from Hampton Research. The precipitant solution consisted of 12% (wt/vol) PEG 4000, 70 mM lithium sulfate, and 100 mM *N*-(2-acetamido)-2-iminodiacetic acid (ADA), pH 6.5. The protein solution contained 2 mg of MAO-B per ml, 8.5 mM Zwittergent 3–12, and 25 mM potassium phosphate buffer, pH 7.5. Crystals of enzyme–inhibitor complexes were obtained by incubating the protein with 2 mM inhibitor followed by gel filtration on Superdex 200. For all

Abbreviation: MAO, monoamine oxidase.

Data deposition: The atomic coordinates and the structure factors have been deposited in the Protein Data Bank, www.rcsb.org (PBD ID codes 1OJA, 1OJB, 1OJC, 1OJD, and 1OJ9).

‡To whom correspondence may be addressed at: (D.E.E.) Department of Biochemistry, Emory University School of Medicine, 1510 Clifton Road, Atlanta, GA 30322. E-mail: dedmond@bimcore.emory.edu; or (A.M.) Department of Genetics and Microbiology, University of Pavia, Via Abbiategrasso, 27100 Pavia, Italy. E-mail: mattevi@ipvgen.unipv.it.

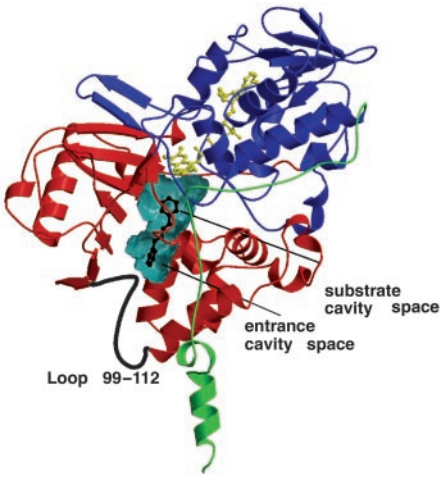

Fig. 1. Overall three-dimensional structure of human MAO-B monomeric unit in complex with 1,4-diphenyl-2-butene. The FAD-binding domain (residues 4–79, 211–285, and 391–453) is in blue, the substrate-binding domain (residues 80–210, 286–390, and 454–488) is in red, and the C-terminal membrane-binding region (residues 489–500) is in green. The FAD cofactor and the inhibitor are shown as yellow and black ball-and-stick models, respectively. The inhibitor binds in a cavity (shown as a cyan surface) that results from the fusion of the entrance and substrate cavities (see text).

inhibitors except tranylcypromine, 2 mM inhibitor was added to the crystallization drop. Triclinic crystals were grown as described (1). X-ray diffraction data were collected at 100 K at the Swiss Light Source in Villigen and at the beam-line ID14-EH4 of the European Synchrotron Radiation Facility in Grenoble, France. The high brilliance provided by these beam-lines resulted in a significant increase of the resolution of the diffraction data. The diffraction images were processed with MOSFLM (8) and programs of the CCP4 package (9).

Structure refinements were performed with the programs REFMAC5 (10) and WARP (11). Tight noncrystallographic symmetry restraints were applied throughout the refinements. The

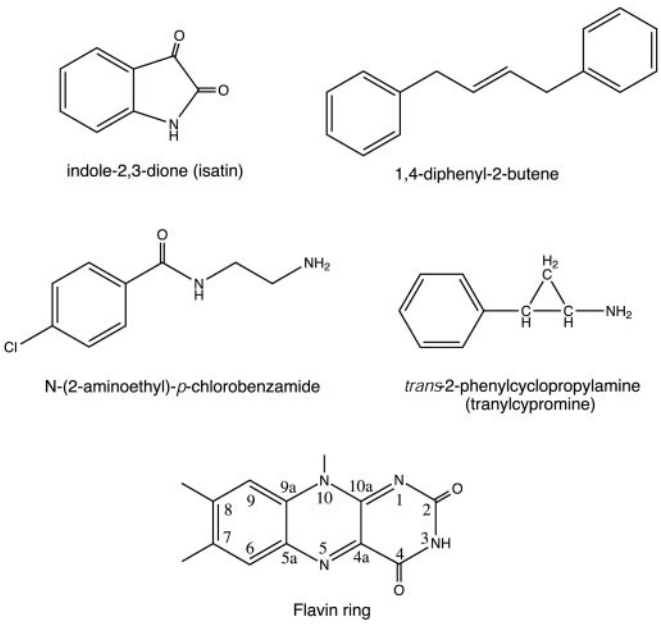

Fig. 2. Structures of MAO-B inhibitors used in this study and atomic numbering of the flavin ring.

atomic models were built with program O (12). Unbiased $2F_o - F_c$ and $F_o - F_c$ maps were used to model the inhibitors which, in all cases, were well defined by the electron density maps (Fig. 3). The models exhibit good stereochemical parameters with only three residues in each monomer (Lys-52, Ala 346, and Asp 419) in disallowed regions of the Ramachandran plot. The refinement statistics are listed in Table 1. Analysis of the final models were carried out with the programs GRID (13) and VOIDOO (14). Pictures were produced by using LIGPLOT (15), BOBSCRIPT (16), MOLSCRIPT (17), and RASTER3D (18).

Results and Discussion

Structural Analysis of Reversible, Noncovalent Inhibitor–MAO-B Complexes. The tight, reversible binding of isatin (Fig. 2) to MAO-B has been known since its original identification (2). Isatin competitively binds to purified, recombinant MAO-B with a K_i of $\approx$3 μM. The tight binding of the inhibitor led to an improved crystal quality and diffraction data could be measured up to 1.7-Å resolution (Table 1). A stereoview of this structure is shown in Fig. 3. The electron density of the dioxoindole ring shows its orientation in the substrate cavity to be perpendicular to the flavin ring with the oxo groups on the pyrrole ring pointing toward the flavin. The 2-oxo group and the pyrrole NH are H-bonded to ordered water molecules present in the active site, whereas the 3-oxo function is not involved in any H-bond. The balance of the binding interactions involve many van der Waals contacts between the isatin ring and amino acid residues in the solvent-inaccessible, hydrophobic substrate cavity.

An unanticipated noncovalent inhibitor of MAO-B was serendipitously discovered when we attempted to determine the structure of the enzyme in the presence of *d*-amphetamine. Rather than containing amphetamine, the crystals were found to contain 1,4-diphenyl-2-butene (whose identification will be detailed in a separate communication, ref. 3). The source of this compound was found to be an impurity released by the polystyrene microbridges used for crystallization of the enzyme. We find that this compound competitively binds to MAO-B ($K_i \approx 35$ μM). Its presence does not interfere with structure determinations of MAO-B in complex with other inhibitors that have higher binding affinities or are covalently bound. The novel aspect of this inhibitor is that it is bound in a manner where one phenyl ring is in the entrance cavity space whereas the other phenyl ring is in the substrate cavity space (Figs. 1 and 4) overlapping the position occupied by isatin. The planes of the two phenyl rings of this inhibitor are orthogonal to one another.

In this structure, the two cavities are now fused into one single cavity, which constitutes a significant proportion of the volume of the protein (Fig. 1). Comparison of the isatin and 1,4-diphenyl-2-butene structures shows that the side chain of Ile-199 exhibits differing rotamer conformations that function as a "gate" between the entrance and substrate cavities (Fig. 5). When isatin is bound, the Ile-199 side chain separates the two cavities. When 1,4-diphenyl-2-butene is bound, the side chain is rotated to a conformation such that the two cavities are no longer separated and are now fused forming a single cavity. This finding of an MAO-B inhibitor that spans both cavities in binding demonstrates that new reversible inhibitors could be developed that would use both cavities as potential binding targets. Unpublished data in our laboratories have shown that *trans-trans*-1,4-diphenyl-1,3-butadiene binds to MAO-B with a higher affinity (K_i = 7 μM). These diphenyl compounds exhibit high specificity for MAO-B (10^3 higher affinity for MAO-B compared with MAO-A) and therefore could represent lead compounds for the development of MAO-B inhibitors.

The concept of cavity-spanning ligands is further supported by analysis of the triclinic MAO-B crystals that were obtained by

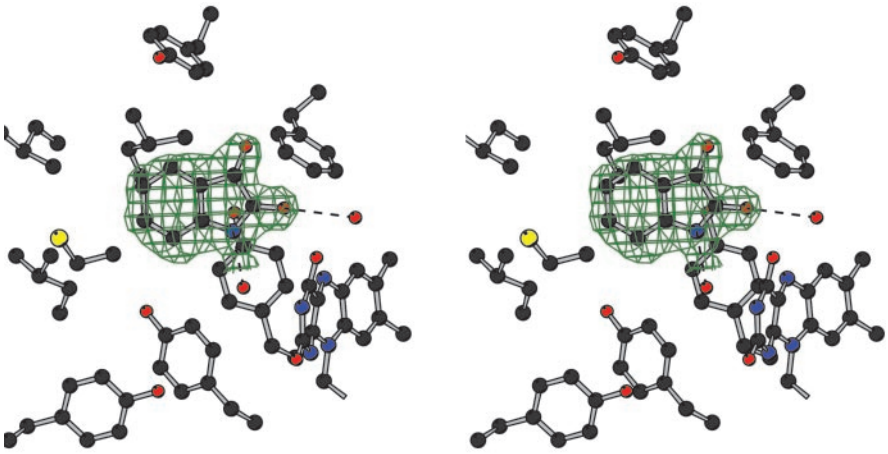

Fig. 3. Stereoview of the isatin binding site and of the $2F_o - F_c$ electron density map calculated at 1.7-Å resolution and contoured at 1-σ level. Carbons are in black, nitrogens in blue, oxygens in red, and sulfurs in yellow. H-bonds involving inhibitor atoms are outlined by dashed lines.

using the detergent lauryldimethylamine *N*-oxide and used for the original structure determination (Table 1) (1). Refinement of this second MAO-B crystal form (*P*1 symmetry with five dimers per unit cell) shows the presence of a detergent molecule bound to each enzyme monomer. The *N*-oxide end of the molecule is positioned near the flavin and the aliphatic side chain traverses the space formerly defined by the substrate and entrance cavities (data not shown).

Structures of Inhibitor-Adducts That Result in a "Bleached" Flavin Spectrum. Two inhibitor classes of MAO-B that have attracted a good deal of attention include the *N*-(2-aminoethyl)arylcarboxamides and *trans*-2-phenylcyclopropylamine (tranylcypromine). Previous studies on the inhibition of MAO-B by lazabemide or *N*-(2-aminoethyl)-4-chlorobenzamide suggest they are oxidized by MAO-B to a form that binds to an active-site amino acid side chain (possibly histidine) in a labile bond that is reduced to a stable bond by treatment with cyanoborohydride (4). Studies of the inhibition of MAO-B with 2-phenylcyclopropylamine concluded that the mode of inhibition was the binding of the oxidation product of MAO-B catalysis to Cys-365 (5, 6).

These studies, as well as spectral studies in our laboratory, show that inactivation of MAO-B by either inhibitor leads to a stable bleaching of the flavin absorption spectrum even in the presence of oxygen. However, in either case, such putative flavin adducts are expected to be labile because denaturation of either inhibited enzyme results in the reappearance of a spectrum characteristic of oxidized flavin. Flavin bleaching is also observed in the crystalline inhibited enzyme as measured by single-crystal microspectrophotometry (data not shown).

The structure of MAO-B after inhibition with *N*-(2-aminoethyl)-4-chlorobenzamide shows that the inhibitor is bound to the enzyme as a flavin N(5) adduct (Fig. 6). The aromatic ring of the inhibitor adopts the same orientation and position as isatin. The resolution of the x-ray data cannot unambiguously determine the detailed molecular formula of this

Table 1. Data collection and refinement statistics

	1,4-Diphenyl-2-butene	Isatin	Tranylcypromine	*N*-(2-aminoethyl)-*p*-chlorobenzamide	Lauryldimethylamine *N*-oxide
Resolution, Å	2.3	1.7	2.2	2.4	3.1
Space group	*C*222	*C*222	*C*222	*C*222	*P*1
Cell, Å	131.1, 224.0, 86.8	130.3, 222.0, 86.0	130.6, 222.5, 86.2	131.7, 223.1, 86.5	108.4, 132.4, 154.8
°	90.0, 90.0, 90.0	90.0, 90.0, 90.0	90.0, 90.0, 90.0	90.0, 90.0, 90.0	90.1, 90.5, 114.0
Unique reflections	49,954	128,815	64,040	47,190	140,447
Completeness, %*	90.6 (66.7)	94.4 (76.7)	99.9 (99.9)	94.5 (85.3)	98.4 (97.8)
Redundancy	5.8	4.3	3.7	3.0	3.8
R_{sym}*†	0.107 (0.202)	0.083 (0.339)	0.130 (0.472)	0.096 (0.303)	0.088 (0.201)
R_{cryst}‡	0.212	0.181	0.206	0.197	0.252
R_{free}‡	0.253	0.204	0.247	0.250	0.260
rmsd bond angle, °	1.2	1.4	1.1	1.1	1.5
rmsd bond length, Å	0.009	0.012	0.007	0.008	0.016
Number of atoms/average *B* factor, Å^2					
Protein + FAD	8,017/43.7	8,017/15.5	8,017/45.4	8,017/19.2	40,139/40.7
Ligand	2 × 16/60.1	2 × 11/17.9	2 × 10/55.1	2 × 13/22.9	10 × 16/35.1
Water molecules	230/39.5	661/27.2	404/29.4	418/21.2	—

rmsd, rms deviation.

*Values in parentheses are for reflections in the highest-resolution shell.

†$R_{sym} = \Sigma|I_i - \langle I\rangle|/\Sigma I_i$, where I_i is the intensity of *i*th observation and $\langle I\rangle$ is the mean intensity of the reflection.

‡$R_{cryst} = \Sigma||F_{obs} - F_{calc}|/\Sigma|F_{obs}|$, where F_{obs} and F_{calc} are the observed and calculated structure factor amplitudes, respectively. R_{cryst} and R_{free} were calculated by using the working and test set, respectively.

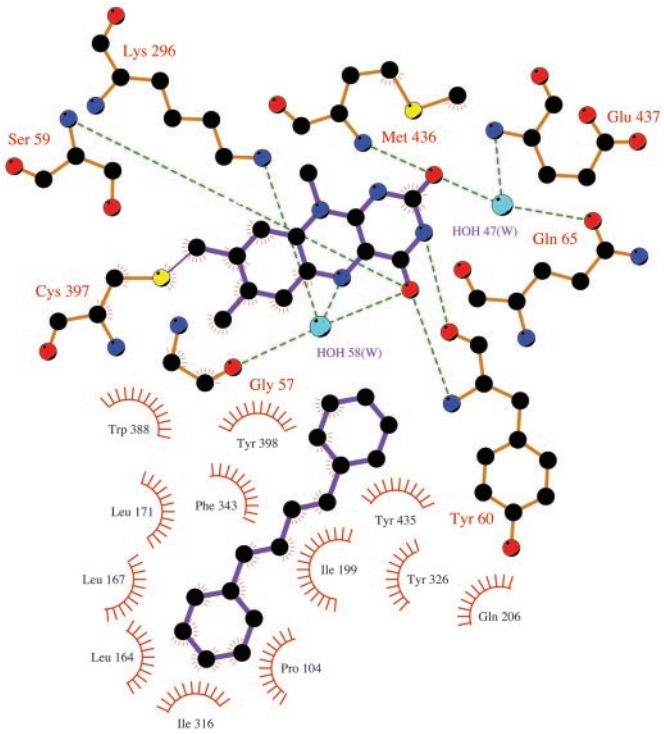

Fig. 4. LIGPLOT (15) illustration of 1,4-diphenyl-2-butene binding to MAO-B. Dashed lines indicate H-bonds. Carbons are in black, nitrogens in blue, oxygens in red, and sulfurs in yellow. Water molecules are shown as cyan spheres.

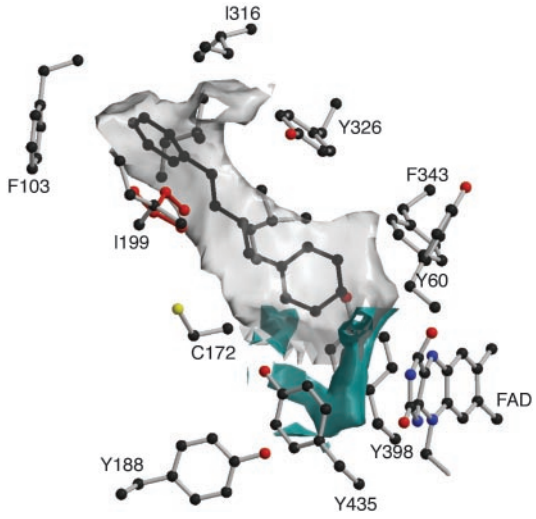

Fig. 5. Isocontour of GRID molecular interaction fields computed with an aromatic sp^2 carbon probe (gray) and with a neutral NH_2 probe (cyan). The contour encloses points with negative values under −2 kcal/mol for the sp^2 carbon probe and −5 kcal/mol for the NH_2 probe. This picture was generated by using the coordinates from the 1,4-diphenyl-2-butene complex with MAO-B. The inhibitor is highlighted in dark gray ball-and-stick; the inhibitor ring in contact with Phe-103, Ile-199, and Ile-316 occupies the entrance cavity space, whereas the inhibitor ring in contact with Tyr-398 and Tyr-435 occupies the substrate cavity space (Fig. 1). Atoms are colored as in Fig. 3. The conformation of Ile-199 as observed in the isatin complex is shown in red to depict the conformational change in this residue that leads to merging of the two cavities, which is observed in the MAO-B complexes with *N*-(2-aminoethyl)-4-chlorobenzamide, 1,4-diphenyl-2-butene, or lauryldimethylamine *N*-oxide.

adduct, as shown in Fig. 7. However, preliminary mechanistic studies of this inhibition suggest the amine nitrogen is released before forming the N(5) adduct. The structural data show that the Ile-199 side chain is in the same rotamer conformation exhibited by 1,4-diphenyl-2-butene such that the entrance and substrate cavities are fused. This change in conformation is necessary to accommodate the *p*-chloro substituent on the benzamide ring.

Structural data of MAO-B inhibited by 2-phenylcyclopropylamine show that this inhibitor binds to the flavin as a C(4a) adduct (Fig. 6). The structure of this adduct differs from that formed with *N*-(2-aminoethyl)-4-chlorobenzamide not only in the flavin ring substitution site but also in the orientation of the phenyl ring, which is parallel to the flavin ring rather than perpendicular as found in all other complexes. To accommodate this ring orientation, Gln-206 must move ≈1 Å. The conformation of the phenyl ring of the tranylcypromine complex does not extend in the substrate cavity far enough to induce the rotamer conformation of Ile-199 to the open form. Thus, in this aspect, the tranylcypromine-inhibited form resembles that of isatin-inhibited MAO-B.

The electron density of the tranylcypromine–MAO-B complex is best fit with a structure in which the cyclopropyl ring is open (Figs. 6 and 7). Formation of this flavin C(4a) adduct can be accommodated by a mechanism for inhibition similar to that shown by Sayre's laboratory for quinone-mediated oxidative cleavage of cyclopropylamines (19). No extra electron density due to inhibitor binding was observed around Cys-365 (see ref. 5) or other sites on the protein. Further work is required for verification of this proposed mechanistic pathway for MAO-B inhibition.

Structural Insights into the Flavin Cofactor of MAO-B. The increased resolution of the x-ray data permits some structural insights for the 8α-*S*-cysteinyl-FAD cofactor of MAO-B. In all structures, an ordered water molecule H-bonds to the N(5) of the flavin and the ε-amino group of Lys-296, which defines a triad [Lys–H_2O–flavin N(5); Fig. 4] also found in the structures of other flavin-dependent amine oxidases (20). A second point to be made is that the peptide bond of the FAD-linking cysteinyl residue (Cys-397–Tyr-398) is in an energetically unfavorable *cis* rather than *trans* conformation. Structural analysis of MAO-B shows that this *cis* Cys-397–Tyr-398 peptide bond results in a favorable steric orientation of the phenolic ring of Tyr-398, which is a component of the active site (1). Examination of structures of other flavoenzymes containing 8α-covalent flavins shows only *trans* conformations of the C-terminal peptide linkage of the residue covalently bound to the flavin. Therefore, this *cis* linkage appears to be unique to MAO-B rather than a general feature associated with covalent binding of flavin coenzymes to proteins. *cis* Nonproline conformers are often found proximal to the functional sites of proteins (21). This strained conformation of the Cys-397–Tyr-398 peptide bond in MAO-B adheres to that paradigm.

Another source of strain about the flavin site is the bent and twisted conformation of the normally flat aromatic isoalloxazine ring of the flavin cofactor (Fig. 6). The angle between the dimethylbenzene ring and the pyrimidine ring is ≈30°. Similarly distorted flavin conformations have been found in other flavin-dependent amine oxidases (20). Structural comparisons of the unsubstituted flavin ring with those of the N(5) and C(4a) adducts of inhibited MAO-B show the flavin ring to exhibit identical conformations. The nonplanar conformation of the oxidized flavin ring structure is expected to facilitate the formation of such adducts because of making the N(5) and C(4a) atoms more sp^3-like in conformation. It is of interest that MAO-B does not conform to the paradigm that flavoprotein oxidases readily form flavin N(5) sulfite adducts. The hydro-

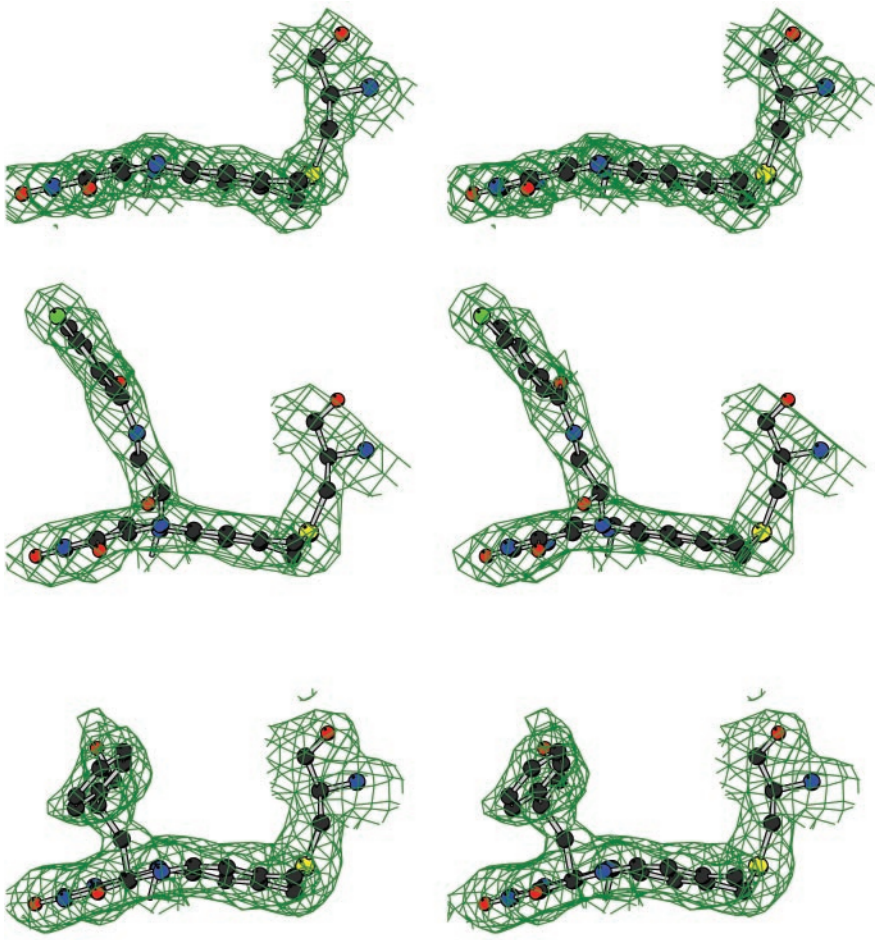

Fig. 6. Crystallographic data of the flavin conformations in MAO-B and in the N(5) and C(4a) adducts. This stereo picture was produced by orienting the flavin ring perpendicular to the plane of the drawing. The electron density (1.7-Å resolution) for the covalently bound flavin in the structure of the isatin complex is shown at *Top*. The *Middle* structure shows the electron density for the covalent adduct with *N*-(2-aminoethyl)-*p*-chlorobenzamide (2.4 Å), and the *Bottom* structure is that formed with *trans*-2-phenylcyclopropylamine (2.2 Å). The contour level is 1 σ.

phobic nature of the entrance and substrate cavities provides a structural rationale for this property. The energetics of an anionic species traversing these hydrophobic cavities are simply too formidable to overcome even though the flavin ring is in a conformation that readily would form such an adduct.

Conclusions Regarding the Active-Site Structure of MAO-B. By using the program GRID (13), a picture of the inhibitor binding site for 1,4-diphenyl-2-butene can be viewed in regards to hydrophobicity and hydrophilicity. As seen in Fig. 5, the major part of the cavity is hydrophobic, which allows for the tight binding of apolar substrates and inhibitors. The only hydrophilic section is near the flavin and is required for recognition and directionality of the substrate amine functionality. This hydrophilic region is located between Tyr-398 and Tyr-435, which, together with the flavin, form an aromatic cage for amine recognition (1, 20). Mutagenesis studies targeting these Tyr side chains in both MAO-A and MAO-B support the key role of these residues in substrate binding (22). We find several ordered, captive water molecules that fill in vacant space in the inhibitor binding cavity. Therefore, the design of future MAO-B inhibitors should consider hydrophilic substituents that could displace these ordered waters, resulting in an increased affinity and specificity. Another aspect emerging from this work are the subtle and inhibitor-dependent changes in conformation of residues in the binding cavity of MAO-B. These results are consistent with conclusions reached from quantitative structure–function activity relationship studies (23) and demonstrate that induced fit and active site plasticity are important components of MAO-B inhibition.

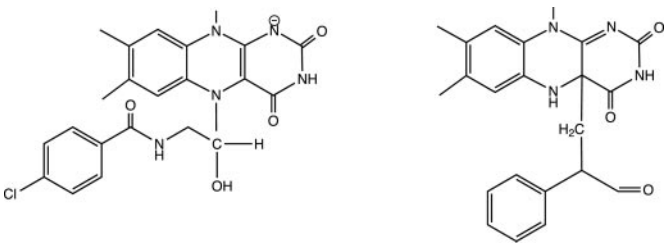

Fig. 7. Proposed structures of the flavin adducts with the MAO-B-catalyzed oxidation products of *N*-(2-aminoethyl)-*p*-chlorobenzamide (*Left*) and of *trans*-2-phenylcyclopropylamine (*Right*).

We thank the staff of the Swiss Light Source and European Synchrotron Radiation Facility for help during x-ray data collection, Ms. Milagros Aldeco for technical assistance with this project, and Dr. A. Mozzarelli (University of Parma) for his assistance with microspectrophotometry experiments. This work was supported by grants from the National Institute of General Medical Sciences (GM-29433), the Ministero dell'Istruzione dell'Universitá e della Ricera (FIRB, COFIN03, and Legge 449/97), and the Agenzia Spaziale Italiana. A.M. and C.B. acknowledge support from a Pfizer Technology Development Support grant.

1. Binda, C., Newton-Vinson, P., Hubálek, F., Edmondson, D. E. & Mattevi, A. (2002) *Nat. Struct. Biol.* **9,** 22–26.
2. Glover, Y. & Sandler, M. (1993) in *Monoamine Oxidase*, eds. Uchida, E., Oguchi, K., Kiuchi, Y. & Yasuhara, H. (VSP, Zeist, The Netherlands), pp. 61–71.
3. Hubálek, F., Binda, C., Li, M., Mattevi, A. & Edmondson, D. E. (2003) *Acta Crystallogr. D*, in press.
4. Cesura, A. M., Gottowik, J., Lahm, H.-W., Lang, G., Imhof, R., Malherbe, P., Röthlisberger, U. & Da Prada, M. (1996) *Eur. J. Biochem.* **236,** 996–1002.
5. Zhong, B. & Silverman, R. B. (1997) *J. Am. Chem. Soc.* **119,** 6690–6691.
6. Paech, C., Salach, J. I. & Singer, T. P. (1980) *J. Biol. Chem.* **255,** 2700–2704.
7. Newton-Vinson, P., Hubálek, F. & Edmondson, D. E. (2000) *Protein Expression Purif.* **20,** 334–345.
8. Leslie, A. G. (1999) *Acta Crystallogr. D* **55,** 1696–1702.
9. Collaborative Computational Project Number 4 (1994) *Acta Crystallogr. D* **50,** 760–767.
10. Murshudov, G. N., Vagin, A. A. & Dodson, E. J. (1997) *Acta Crystallogr. D* **53,** 240–255.
11. Morris, R. J., Perrakis, A. & Lamzin, V. S. (2002) *Acta Crystallogr. D* **58,** 968–975.
12. Jones, T. A., Zou, J. Y., Cowan, S. W. & Kjeldgaard, M. (1991) *Acta Crystallogr. A* **47,** 110–119.
13. Kastenholz, M. A., Pastor, M., Cruciani, G., Haaksma, E. E. & Fox, T. (2000) *J. Med. Chem.* **43,** 3033–3044.
14. Kleywegt, G. J. & Jones, T. A. (1994) *Acta Crystallogr. D* **50,** 178–185.
15. Wallace, A. C., Laskowski, R. A. & Thornton, J. M. (1995) *Protein Eng.* **8,** 127–134.
16. Esnouf, R. M. (1999) *Acta Crystallogr. D* **55,** 938–940.
17. Kraulis, P. J. (1991) *J. Appl. Crystallogr.* **24,** 946–950.
18. Merritt, E. A. & Bacon, D. J. (1997) *Methods Enzymol.* **277,** 505–524.
19. Sayre, L. M., Singh, M. P., Kokil, P. B. & Wang, F. (1991) *J. Org. Chem.* **56,** 1353–1355.
20. Binda, C., Mattevi, A. & Edmondson, D. E. (2002) *J. Biol. Chem.* **277,** 23973–23976.
21. Herzberg, O. & Moult, J. (1991) *Proteins Struct. Funct. Genet.* **11,** 223–229.
22. Geha, R. M., Chen, K., Wouters, J., Ooms, F. & Shih, J. C. (2002) *J. Biol. Chem.* **277,** 17209–17216.
23. Walker, M. C. & Edmondson, D. E. (1994) *Biochemistry* **33,** 7088–7098.